Nanometer-sized structures and the transition from the molecular to the solid state

Georgia C. Papaefthymiou
Francis Bitter National Magnet Laboratory, Massachusetts Institute of Technology, Cambridge, Massachusetts 02139
(Received 13 April 1992; revised manuscript received 29 June 1992)

The magnetic properties of nanometer-sized molecular complexes that contain an increasing number n of superexchange-coupled iron ions ($10 \leq n \leq 20$) participating in three-dimensional or lower-dimensional magnetic interactions are examined. The experimental criteria that establish the onset of incipient solid-state magnetic correlation effects in these molecules are emphasized. These chemical structures are beyond the molecular realm but convergence to the bulk has not yet been attained. Thus, they afford appropriate experimental systems to test theoretical predictions that the onset of incipient solid-state phenomena—such as the emergence of a conduction band in metallic clusters and collective magnetic interactions responsible for magnetic ordering in solids—occurs in the vicinity of $n \geq 10$, where n is the number of atoms or interacting spins in the cluster.

I. INTRODUCTION

Cluster science is a fairly young discipline that concerns itself with the molecular–solid-state phase boundary, with impact on a diverse number of subdisciplines of chemistry, physics, and materials science. The electronic and magnetic properties of small (<10 Å in diameter) metallic clusters, for example, have been of considerable interest because of commercial applications in heterogeneous catalysis[1] and high-density magnetic memory,[2] and because of an intrinsic interest in how they relate to the bulk band structures and surface states of the corresponding crystalline metals. Semiconductor nanostructures are of intense current interest because of their potential use in the emerging field of nanotechnology.[3]

The quantum-mechanical description of metallic clusters has been rigorously pursued[4] since the mid-1970s while experimental observations have appeared only since the mid-1980s, primarily due to the rapidly developing field of cluster beams.[5] Molecular orbital calculations by Messmer *et al.*[6] using self-consistent-field-Xa scattered-wave methods on Cu, Ni, Pd, and Pt clusters indicate a fast convergence of the discrete energy levels associated with the molecular state to the electronic density of states for the corresponding crystalline metals obtained through band-structure calculations. They predict that a cluster of only 13 Cu atoms already possesses an electronic structure similar to that of the extended solid. They also indicate that Ni_8 and Ni_{13} clusters are magnetic, while Pd_{13} and Pt_{13} are not, consistent with the behavior found in the bulk metals.

Calculations on iron clusters by Yang *et al.*[7] show that the dominance of magnetic effects on the electronic structure is quickly established. For Fe_{15} all of the major features of the bulk density of states are present in the cluster. Spin-density maps generated for Fe_{15} bear a striking resemblance to those derived from neutron-scattering experiments on bulk iron.[8] They also show features that are absent in the extended solid or the molecular state. Recent experimental efforts to control the size and dimensionality of materials by growing them as clusters, multilayered, and modulated structures[9] have, indeed, produced systems with unusual electronic and magnetic properties exhibiting quantum-size effects.

A number of experimental studies of the development of the electronic band structure of a solid with increasing cluster size have appeared in the literature with results generally confirming theoretical predictions.[10] In contrast, experimental investigations of the magnetic properties of metallic clusters have been rather limited.[11,12] Direct experimental observation of collective magnetic interactions—that is, short-range intracluster magnetic ordering—in one-nanometer-diameter clusters has been hindered by the difficulty of obtaining isolated, well-characterized metallic clusters of such extremely small and uniform size.

Large molecular complexes,[13–16] like clusters, lie at the boundary between the molecular and the solid state but are structurally well characterized and crystallographically isolated, providing experimental systems appropriate for the investigation of the onset of collective magnetic phenomena associated with the solid state. With the caveat that the magnetic structure of metallic clusters is determined through direct *d-d* exchange interactions between atoms, while in molecular complexes magnetic ions interact through indirect superexchange via intervening ligands, their study constitutes a separate approach from that of elemental cluster beams to the much debated subject of the transition from the molecular to the solid state. Furthermore, this approach has produced chemical structures where interactions between magnetic ions are confined in a plane or a chain, which constitute finite analogs of lower-dimensional magnetic solids.[17–21]

In the solid-state magnetic exchange, magnetic anisotropy and magnetic dimensionality are important factors in the process of magnetic ordering. Most lower-dimensionality magnetic solids do not undergo long-range order until very low temperatures are realized, when the weak interchain or interlayer exchange forces

become important enough to drive three-dimensional (3D) ordering. Above this temperature, interesting short-range-order correlation phenomena may be observed.[22] Crystallographically isolated molecular clusters of an increasing number of exchange-coupled ions confined in a plane or in a chain may serve as finite analogs of pure 2D or 1D magnetic systems and may exhibit interesting short-range correlation effects, such as spin-wave excitations.[23] Indeed, a great deal of the theoretical work in 1D magnetic systems has been done on hypothetical finite antiferromagnetic chains or rings.[24–26] Theoretical calculations of the spin-wave spectra of the antiferromagnetic linear chain[24] indicate fast convergence to the system of the infinite chain for $n \geq 10$ where n is the number of interacting spins in the chain. To date no experimental confirmation of these predictions has been obtained.

Such experimental confirmation presents a special challenge to the experimentalist, however, due to superparamagnetic-relaxation[27,28] and spin-fluctuation[29] phenomena, which result in very short spin-relaxation times τ_s. Thus, the observation of the onset of magnetic-ordering phenomena in nanometer-sized macromolecular structures depends critically on the characteristic measuring time τ_m associated with the particular experimental technique used. A fast spectroscopy is required with $\tau_m \ll \tau_s$ and ultralow sample temperatures.

Iron complexes have been chosen as experimental test systems because their magnetic properties can be studied not only by magnetic susceptibility measurements, but also by Mössbauer spectroscopy. The characteristic measuring time for Mössbauer spectroscopy is $\tau_{\text{Möss}} \sim 10^{-8}$ sec, while that for magnetic susceptibility measurements is often $\tau_{\text{mag}} \sim 1$ sec. Thus, Mössbauer spectroscopy can probe dynamical spin-fluctuation phenomena while susceptibility studies give only averaged magnetic-moment information. This approach has led to the experimental study, briefly addressed earlier[14,21] and fully presented here, which has allowed confirmation of theoretical predictions that collective magnetic phenomena, responsible for magnetic ordering in solids, first appear in the vicinity of $n \approx 10$, where n is the number of interacting spins in a 3D cluster. In contrast, clusters of lower magnetic dimensionality containing up to twenty exchange-coupled iron ions have failed to produce such correlation effects within the Mössbauer time window at temperatures down to 1.6 K.

II. MATERIALS

A. Molecular clusters of 3D magnetic dimensionality

Iron polymerization in aqueous solutions results in the uncontrollable formation of mixtures of high-molecular-weight polymers.[30] The generation of monodispersed oxo-hydroxo-iron nanoclusters requires a competitive reaction chemistry between core cluster growth to form a bulk material and cluster encapsulation by terminal ligation that arrests further core growth. By using aprotic solvents as the reaction medium and adding water, needed for hydrolysis, and an organic base in limited quantities, a certain degree of control of the extent of polymerization and resulting size of the clusters can be achieved. Structurally characterized complexes of nuclearity Fe_3, Fe_4, Fe_6, Fe_8, and Fe_{11} made of $[Fe_2O]^{4+}$ and $[Fe_3O]^{7+}$ building blocks have been reported in the literature.[31] These complexes have been investigated as possible intermediates[14] in a biomimetic approach to the study of the iron nucleation process by ferritin, the iron storage protein in mammalian and bacterial life forms.[32] In this case, encapsulation of the iron-oxo-hydroxo mineral phase in nanometer-sized particulate form is done by the protein shell.

The structure of the undecanuclear complex $[Fe_{11}O_6(OH)_6(O_2CPh)_{15}]\cdot 6THF$ (cluster 1) is shown in Fig. 1. All metal atoms are six coordinated, of distorted octahedral symmetry, and all donor atoms are oxygen from oxo, hydroxo, and benzoate groups where the latter surround and encapsulate the central iron-rich core. Further polymerization of this structure has provided large mixed-metal, mixed-valence complexes of the form $[Fe_{16}MO_{10}(OH)_{10}(O_2CPh)_{20}]$, where M is a divalent transition-metal ion. Structures with $M = Mn^{2+}$, Co^{2+}, and Fe^{2+} have been isolated. Figure 2 shows the structure of the $[Fe_{16}Mn]$ (cluster 2) cluster. The structure is centrosymmetric with a Mn^{2+} ion located at the center of symmetry. This Mn^{2+} ion forms the shared corner of an $[Fe_3O_3(OH)]_2Mn$ double cube which is surrounded by an $[Fe_{10}O_4(OH)_8]$ cage, and this, in turn, is encapsulated within a shell of 20 benzoate ligands. Further details on the synthesis and x-ray structure of these molecules have been reported previously.[13–15]

These are neutral molecules forming crystals by van der Waals forces. The bulky benzoate ligands that encapsulate the central exchange-coupled ion cores, which are about 10 Å in diameter, keep the cores magnetically isolated from one another at an average distance between centroids of ~20 Å. (See Fig. 3.) Thus, any magnetic-

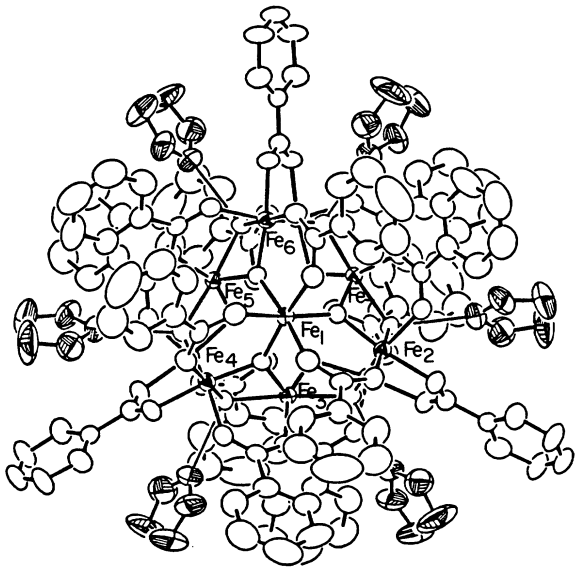

FIG. 1. Crystal structure of $Fe_{11}O_6(OH)_6(O_2CPh)_{15}\cdot 6THF$ (cluster 1) showing 40% probability thermal ellipsoids. Only 7 of the 11 Fe ions are discernible in this view of the molecule.

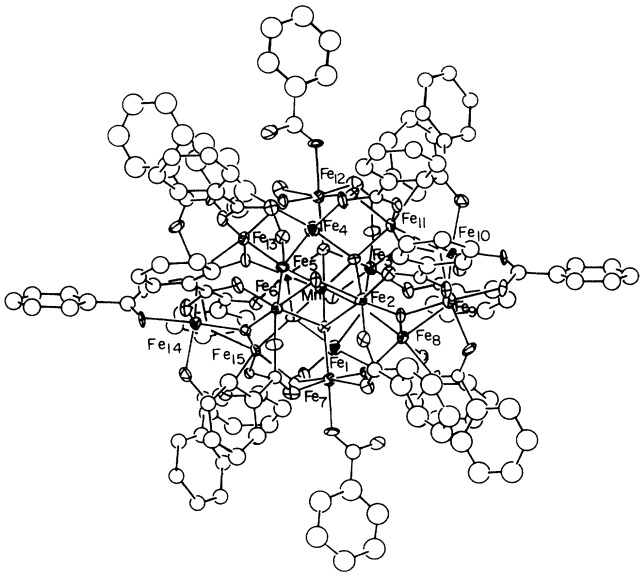

FIG. 2. Crystal structure of $Fe_{16}MnO_{10}(OH)_{10}(O_2CPh)_{20}$ (cluster 2) showing 20% probability thermal ellipsoids. Only 15 of the 16 Fe atoms are discernible.

ordering effects observed should be due to intramolecular spin interactions rather than long-range magnetic order throughout the crystal *(vide infra)*.

B. Molecular clusters of low magnetic dimensionality

Iron sulfur chemistry has also led to the synthesis of macromolecular structures where Fe is tetrahedrally coordinated to sulfur atoms and arranged in lower-dimensional magnetic structures.[17] The fundamental building block in these systems is the

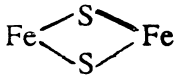

rhomb. The fusion of such rhombs by edge- and vertex-sharing leads to the production of polymeric iron sulfur structures,[17] a number of which are lower dimensional.

The highest nuclearity FeS cluster produced to date by self-assembly reactions in nonaqueous solvents is the cluster $[Na_2Fe_{18}S_{30}]^{8-}$ (cluster 3) shown in Fig. 4. It has a disklike topology with dimensions 13.3×16 Å, maximum thickness of 3.3 Å, and no terminal ligation. The structure closes upon itself, obviating the need for terminal ligation to arrest further growth, a situation, albeit of lower dimensionality, analogous to that of the resonant closed-shell structures of the fullerene carbon molecules.[33] All iron ions in cluster 3 are confined in a plane. Two sodium ions are bound to the interior sulfur atoms of the cluster, partially balancing out the high negative electronic charge on the $Fe_{18}S_{30}$ ring. The cluster is stabilized as the anion in the crystal $(Pr_4N)_6Na_4Fe_{18}S_{30}\cdot 14MeCN$. The crystal structure consists of discrete Pr_4N^+ ions and two additional Na^+ ions weakly associated with cluster 3. Further details on the synthesis and structure of this complex have been reported elsewhere.[17] The ring molecules pack in the ionic crystal with only translational symmetry, which results in parallel layers of anions similar to those found in many chalcogenide binary phases. (See Fig. 5.) The average distance between ring molecules is also about 20 Å. This system can serve as a finite analog of extended lower-magnetic-dimensionality layered structures.

Analogous FeSe chemistry has led to the production of another closed chemical structure, an unprecedented Fe_{20} cluster[19,20] of stoichiometry $[Na_9Fe_{20}Se_{38}]^{9-}$ (cluster 4) shown in Fig. 6. It has a bicyclic structure of ellipsoidal shape. The structure is built up from Fe_2Se_2 rhombs, which form three short linear FeSe segments connected together at the ends by vertex sharing and edge fusion. Nine sodium ions are encapsulated within the cluster cavity. The cluster approaches D_{3h} symmetry with a pseudo-C_3 axis along the Fe(10)-Fe(10′) vector. Cluster dimensions are 17.4 Å [Se(1)-Se(1′)]×11.2 Å (2[centroid-Se(6)]). The resulting structure, while topologically three dimensional, represents a rare example of a finite 1D magnetic system. Iron ions are strongly ex-

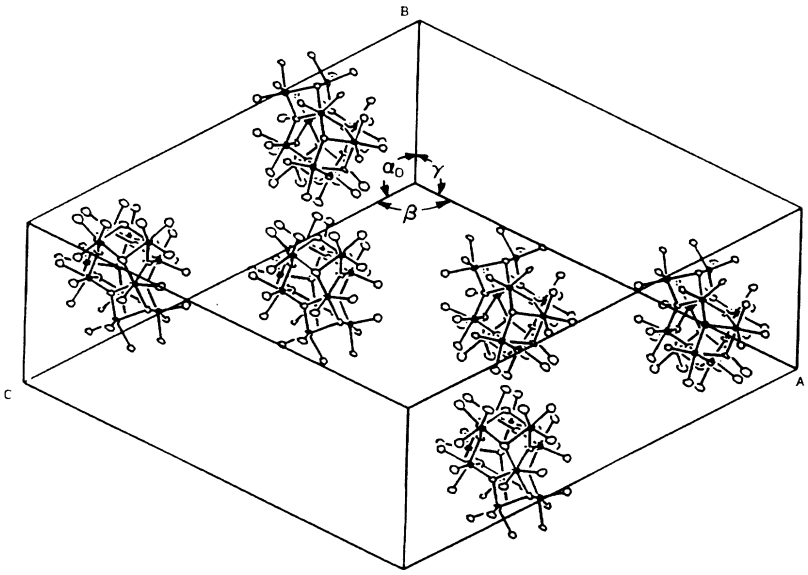

FIG. 3. Crystal packing of Fe_{11} clusters. Only the inner magnetic cores $[Fe_{11}O_6(OH)_6]^{15+}$ of the clusters are shown. Unit cell: $a=28.5$ Å, $b=18.6$ Å, $c=29.9$ Å, $\alpha=90°$, $\beta=115.9°$, $\gamma=90°$. Average distance between cluster centroids ~20 Å.

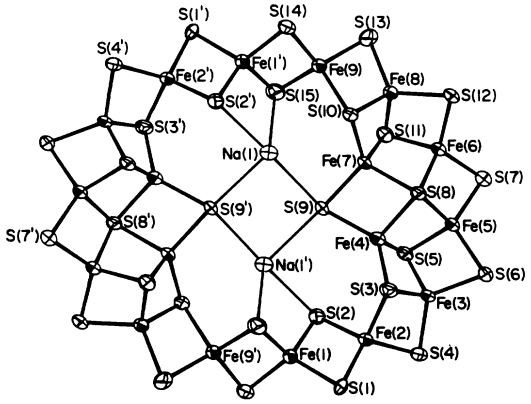

(a)

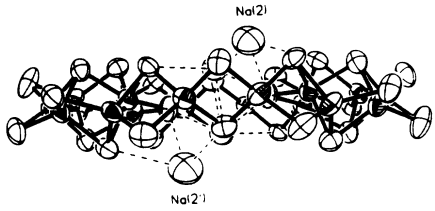

(b)

FIG. 4. (a) Structure of $[Na_2Fe_{18}S_{30}]^{8-}$ (cluster 3) showing 50% probability ellipsoids. Primed and unprimed atoms are related by an inverse center. (b) Side view of the molecule.

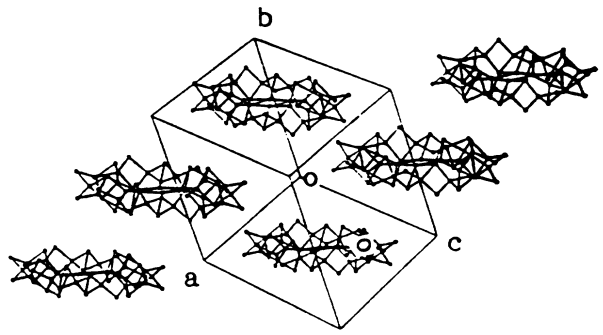

FIG. 5. Stacking of the $Fe_{18}S_{30}$ rings in the crystal. There is an approximately 20-Å distance between the centroids of adjacent rings.

change coupled through the bridging Se atoms along linear segments, but lack any bridging atoms between chains. The cluster is stabilized within an ionic crystal with stoichiometry $(Bu_4N)_{4.5}Na_{13.5}Fe_{20}Se_{38}\cdot 2PhNHCOMe\cdot 15EtOH$. Further details on the synthesis and structure are given elsewhere.[19,20]

III. EXPERIMENTAL METHODS

Magnetization measurements were performed with a superconducting quantum interference device magnetometer in the temperature range $1.8 \leq T \leq 300$ K and applied field range $0 \leq H_o \leq 50$ kOe and by use of a Foner vibrating sample magnetometer (VSM) associated with the Bitter electromagnet high-field facility at the Francis Bitter National Magnet Laboratory affording applied magnetic fields up to 230 kOe.

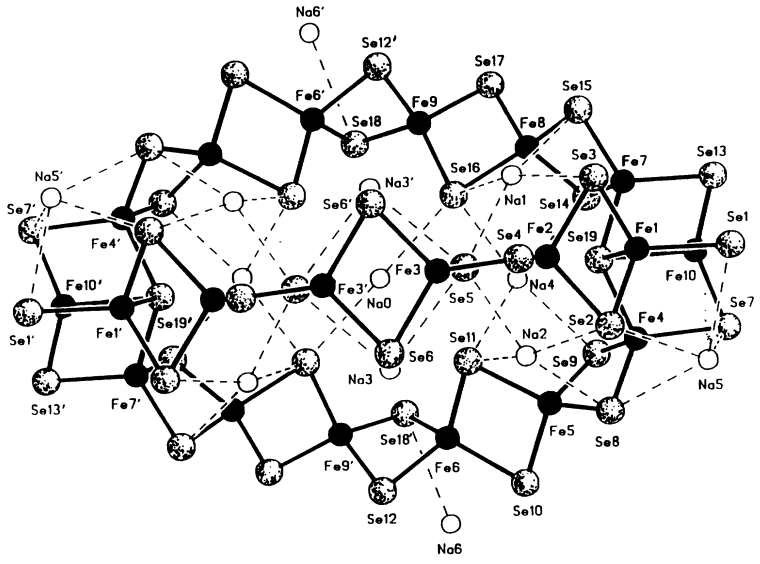

(a)

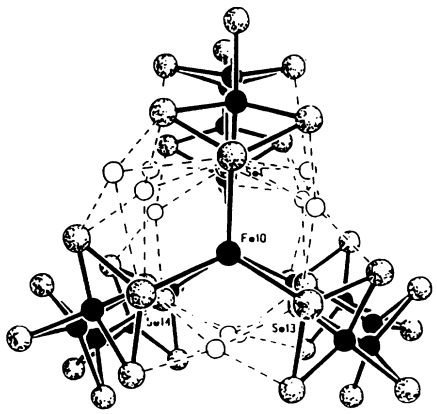

(b)

FIG. 6. (a) Structure of $[Na_9Fe_{20}Se_{38}]^{9-}$ (cluster 4). Primed and unprimed atoms are related by an imposed C_2 axis passing through Na(0) and perpendicular to the $Fe_2(3,3')Se_2(6,6')$ rhomb. (b) Depiction of the pseudo-C_3 axis along the Fe(10)-Fe(10') vector.

Mössbauer measurements were performed with a conventional constant acceleration spectrometer with variable temperature, $1.8 \leq T \leq 300$ K, and a longitudinal applied magnetic field, $0 \leq H_o \leq 80$ kOe, capability. This technique probes the local moments at the iron nuclei, the degree of charge and spin localization (or delocalization), dynamical spin-relaxation[27–29,34] processes, magnetic anisotropy, spin canting, and spin reorientation phenomena.[35,36] Experimental spectra were fit using standard fitting procedures to theoretical spectra, including distribution of internal magnetic fields. Isomer shifts are given relative to metallic iron at room temperature.

IV. RESULTS AND DISCUSSION

Variable-temperature magnetic-susceptibility studies for clusters 1 and 2 showed paramagnetic behavior. A sharp increase in μ_{eff} with temperature was observed indicative of a net antiparallel spin coupling within the aggregate $[Fe_{11}]$ and $[Fe_{16}Mn]$ molecular cores and the existence of low-lying magnetic excited states.[37] Extrapolation of μ_{eff} values to zero temperature gives $\sim 1.9\mu_B$ and $\sim 5.9\mu_B$ per cluster for clusters 1 and 2, respectively, approximating a ground electronic net or total spin state for complex 1 of $S_T = \frac{1}{2}$ and for 2 of $S_T = \frac{5}{2}$ by use of the relationship $\mu_{\text{eff}} = [g^2 S(S+1)]^{1/2}$ and assuming $g = 2$. At room temperature the effective moment for cluster 1 has saturated at a value of $14.6\mu_B$ per molecule while for cluster 2, $\mu_{\text{eff}} \sim 13.5\mu_B$ per molecule and still increasing.

High-field magnetization studies using a VSM magnetometer in a water-cooled Bitter electromagnet up to 230 kOe, reveal a monotonic increase of cluster moments up to the highest field without reaching saturation [Figs. 7(a) and 7(b)]. There is no hysteresis in the magnetization, and no remnant moment for either cluster when the field is swept up to 230 kOe and back down to zero. An interesting step in the magnetization vs applied-field functional dependence reminiscent of a spin-flop magnetic phase transition[38] is observed for cluster 1 which is absent in cluster 2 *(vide infra)*.

Mössbauer spectra of polycrystalline samples at $T = 80$ K are paramagnetic and show a symmetric quadrupole doublet with an isomer shift $\delta = 0.50$ mm/sec and a quadrupole splitting $\Delta E_Q = 0.91$ mm/sec for the $[Fe_{11}]$ cluster and $\delta = 0.51$ mm/sec, $\Delta E_Q = 0.77$ mm/sec for the $[Fe_{16}Mn]$ cluster, typical of high spin $S = \frac{5}{2}$, Fe^{3+} ions. The isomer shifts are comparable to those of oxo-bridged high-spin ferric complexes, but the quadrupole splittings are smaller than those observed for oxo-bridged complexes (1.5–2.0 mm/sec) (Ref. 39) and approach those reported for iron-oxide and iron-hydroxide particles.[40–42].

At 4.2 K the Mössbauer spectrum of compound 1 is dominated by intermediate relaxation phenomena (Fig. 8). It is significantly broadened, with wings that extend from about -7 to $+7$ mm/sec, but no magnetic hyperfine lines are defined even at 1.8 K. The net moment of the Fe_{11} aggregate does not have a fixed spatial orientation in zero field but fluctuates with a certain frequency with respect to the crystal axis. The broadening of the Mössbauer spectrum implies that the relaxation time is of the order of the Mössbauer time scale. In contrast, compound 2 exhibits relaxation phenomena in its Mössbauer spectra, appearing at $T \cong 7$ K, with magnetic hyperfine lines developing below 6 K, superimposed on a broad absorption envelope at the center of the spectrum (Fig. 9). With decreasing temperature the intensity of the magnetic subspectrum increases at the expense of the central doublet. At 1.8 K, a well-defined magnetic, six-line absorption spectrum is obtained, indicating that the complex has crossed from fast to slow spin-relaxation behavior on the Mössbauer time scale.

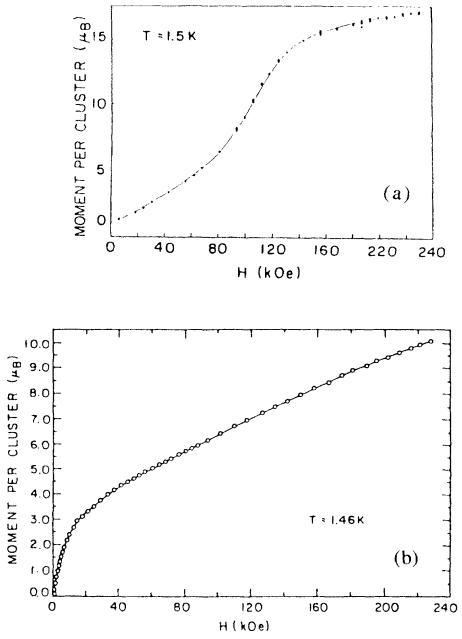

FIG. 7. High-field magnetization of (a) $[Fe_{11}O_6(OH)_6(O_2CPh)_{15}]\cdot 6THF$ and (b) $[Fe_{16}MnO_{10}(OH)_{10}(O_2CPh)_{20}]$.

Figures 10 and 11 show spectral behavior in the presence of an external magnetic field $\mathbf{H}_o$ of 60 and 80 kOe applied parallel to the direction of the 14.4-keV γ ray for compounds 1 and 2, respectively. In the presence of the

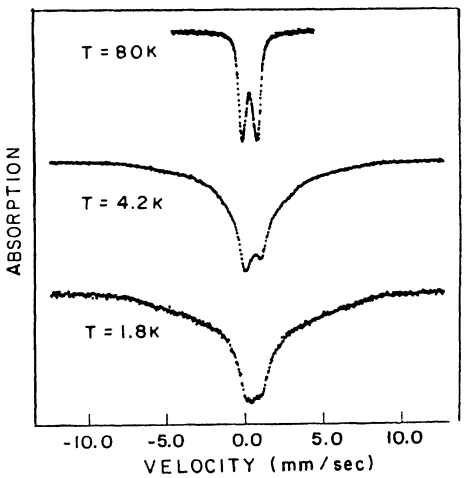

FIG. 8. Mössbauer spectra of polycrystalline $[Fe_{11}O_6(OH)_6(O_2CPh)_{15}]\cdot 6THF$ at various temperatures.

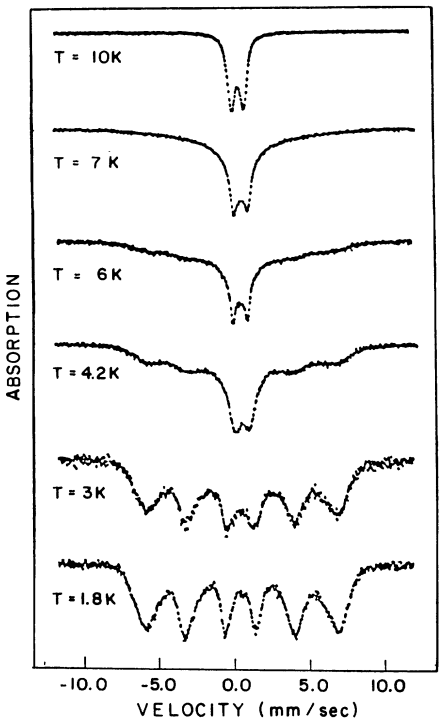

FIG. 9. Mössbauer spectra of polycrystalline $[Fe_{16}MnO_{10}(OH)_{10}(O_2CPh)_{20}]$ at various temperatures.

field, the total spin of the cluster is forced to precess about $\mathbf{H}_o$, further reducing its relaxation time. Thus, while at 4.2 K in zero field, both compounds 1 and 2 exhibit a strong absorption doublet at the center of the spectrum (Figs. 8 and 9), at the same temperature upon application of the field only magnetically split spectra are

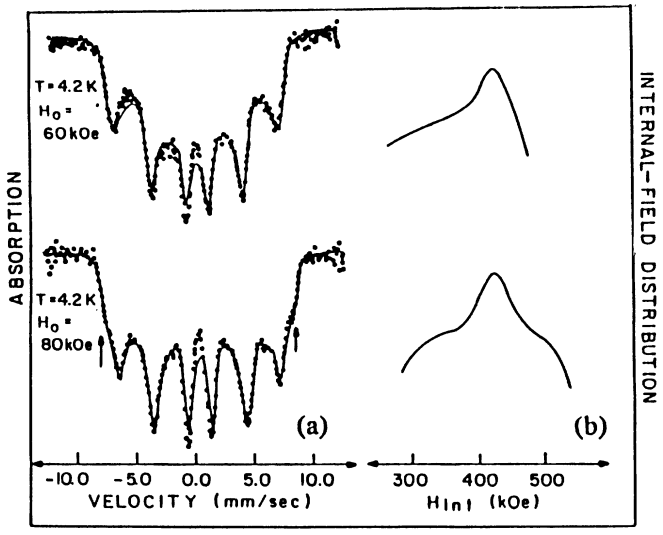

FIG. 10. (a) Low-temperature Mössbauer spectra of cluster 1 in external magnetic fields H_o parallel to the γ-ray direction. The solid line is a least-square fit of the experimental data to a distribution of internal magnetic fields. (b) The resulting distribution of internal magnetic fields at the sites of the iron nuclei.

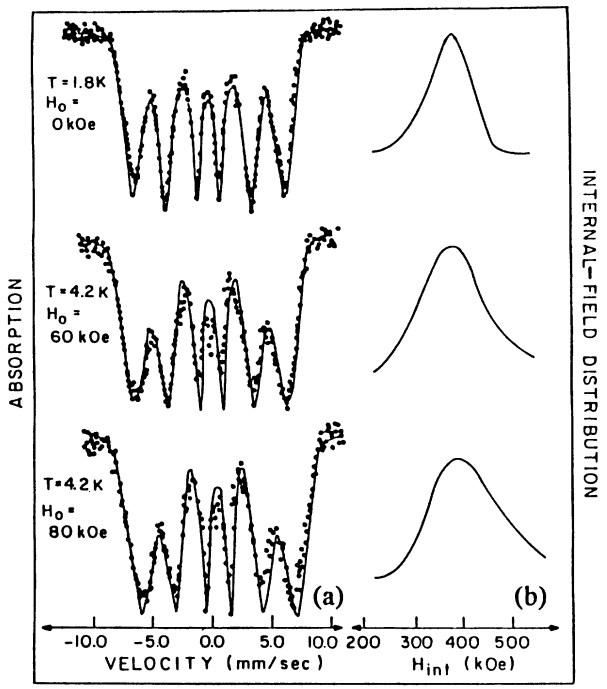

FIG. 11. (a) Low-temperature Mössbauer spectra of cluster 2 in the absence and presence of a longitudinal external magnetic field H_o. The solid line is a least-square fit of the experimental data to a distribution of internal magnetic fields. (b) The resulting distribution of internal magnetic fields at the sites of the iron nuclei.

observed (Figs. 10 and 11). The six lines in each spectrum correspond to the two $\Delta m = 0$ (lines 2 and 5) and the four $\Delta m = \pm 1$ lines of a magnetic hyperfine spectrum.[42] It is most notable that (a) upon application of the external field the middle $\Delta m = 0$ absorption lines persist and (b) the overall magnetic splitting, which is a measure of the total effective magnetic field at the iron nucleus, does not change significantly with increasing applied field.

The Mössbauer spectra in the presence of the external field provide the means of distinguishing between slow paramagnetic relaxation and magnetic ordering. The simplest example of the interaction between two magnetic ions is that which occurs in a dimer complex. The principle interaction of magnetic exchange, $\mathcal{H}_{ex} = -J\mathbf{S}_1 \cdot \mathbf{S}_2$, is short range and results in parallel or antiparallel spin alignment within the molecular complex.[38] In a three-dimensional crystalline lattice, however, the same pairwise exchange interaction leads to the transition from the paramagnetic state to a magnetically ordered state with long-range correlation between magnetic moments.[43] In the study of paramagnetism the only preferred direction for spin polarization is that of the applied field, while in magnetic solids easy axes of magnetization within the crystalline structure determine the direction of local spin orientation until high enough fields are applied that overcome internal magnetic anisotropy energies.[43]

Molecular complexes containing an even number of exchange-coupled high-spin ferric ions produce simple Mössbauer spectra in the presence of an applied field,

typical of diamagnetic complexes[44] where the only field at the iron nuclei is that of the applied field $\mathbf{H}_o$. Complexes containing an odd number of exchange-coupled high-spin ferric ions produce complex Mössbauer spectra[45] governed by the Hamiltonian $\mathcal{H}=\mathcal{H}_{ex}+g\beta\mathbf{H}_o\cdot\langle\mathbf{S}_T\rangle -g_n\beta_n\Sigma_i\mathbf{I}_i\cdot\mathbf{H}_{ni}$, where $\langle\mathbf{S}_T\rangle$ is the expectation value of the total electronic spin of the cluster, produced by the strong intracluster exchange interaction $\mathcal{H}_{ex}$, and $\mathbf{H}_{ni}$ is the total magnetic field at the ith nucleus of nuclear spin $\mathbf{I}_i$. All other symbols have their usual meaning. The second term gives the electronic and the third the nuclear Zeeman interaction, where the total magnetic field at the ith nucleus $\mathbf{H}_{ni}$ is given by the vector sum of the applied $\mathbf{H}_o$, and hyperfine magnetic field $\mathbf{H}_{hfi}$, due to the unpaired $3d$ electrons.[42] Because high-spin ferric ions are highly isotropic, local spins project along the direction of the total spin of the cluster $\mathbf{S}_T$ which, in turn, projects in the direction of the applied field, producing total internal fields at the iron nuclei colinear with $\mathbf{H}_o$ and, therefore, with the γ-ray propagation direction. Selection rules for the magnetic dipole Mössbauer transition then dictate that the $\Delta m=0$ lines (lines 2 and 5) approach zero intensity.[42]

The nonvanishing $\Delta m=0$ lines in Figs. 10 and 11 indicate that even though the total moment of the cluster may be aligned along the direction of the magnetic field, the hyperfine fields and, therefore, the local magnetic moments, at the different iron sites are not colinear with the total moment or $\mathbf{H}_o$, but tend to lie perpendicular to it and, therefore, to the total spin of the cluster. That is, internal magnetic anisotropies dominate. Their presence points to collective magnetic interactions producing short-range magnetic ordering and the existence of easy directions of magnetization within the crystalline solid. They point to a noncolinear antiferromagnetic structure or canted antiferromagnetic order of the type observed in oxidic spinels[46] or the surface atoms of antiferromagnetic small particles.[35] In a cluster containing a number of the order of ten interacting spins, almost all spins lie on the surface and surface effects should dominate. It could also be a result of frustration in the network of magnetic interactions present resulting in a spin-glass-like structure.[47] There is no long-range spatial correlation of the antiferromagnetic axis of a cluster with its neighbors, since clusters are separated by a distance of $\sim$20 Å, over which long-range dipole-dipole interactions are negligible.[48] Thus, the magnetic domain size must be confined within the Fe_{11} or $Fe_{16}Mn$ core. A broad transition to a six-line absorption spectrum is observed in the zero-field Mössbauer spectra of $Fe_{16}Mn$ (Fig. 9) superimposed on a relaxation envelope. The positions of the outer absorption lines, which give a measure of the observed hyperfine magnetic field $H_{hf}\sim 400$ kOe, are independent of temperature, a behavior reminiscent of the superparamagnetism of single-magnetic-domain particles (<100 Å) of antiferromagnetically coupled ferric oxides and hydroxides.[40,41]

Let us compare the results shown in Fig. 9 with those of magnetically ordered fine particles.[35,40,41] The magnetic moment of ultrafine particles undergoes, above a certain temperature, spontaneous reversals, analogous to the behavior of paramagnetic atoms, exhibiting the so-called superparamagnetic behavior.[27,28] The relaxation time $\tau_s=\tau_0\exp(2KV/k_BT)$ where K is the magnetic anisotropy constant, V is the volume of the particle, k_B is Boltzmann's constant, and T is the temperature. τ_0 is a constant characteristic of the material of the order of the 10^{-9} sec.[40] The Mössbauer spectrum of a system where τ_s is fast with respect to the Mössbauer time scale is a doublet, while that of a slow relaxing system is a sextet. The characteristic time $\tau_{Möss}$ is given by the ^{57}Fe nuclear-spin Larmor precession time τ_L of the 14.4-keV energy state in the hyperfine field at the nucleus. For $H_{hf}\sim 400$ kOe, as observed for compound 2, $\tau_L\approx 3.2\times 10^{-8}$ sec. The temperature at which the system changes from the fast to the slow relaxation regime, i.e., at $\tau_s=\tau_L$, is known as the blocking temperature T_B for the Mössbauer technique. For cluster 2, analysis of the temperature dependence of the Mössbauer spectra gives $T_B\approx 4$ K, while for cluster 1, $T_B<1.8$ K.

The basic difference between the present Mössbauer study of well-defined molecular clusters, and thus of a single volume, and those of fine particles available in the literature[40,41] is that the latter deal with a broad distribution of particle sizes giving rise to very broad transitions from the doublet to the six-line spectrum. The breadth of the transition has often been used to determine the distribution of particle sizes present in the sample, assuming an infinitely sharp transition for each particle volume.[40] Theory predicts, however, that, as observed here, even single-particle volume samples may exhibit transitions that are narrow but of finite sharpness, the latter being inversely proportional to the saturation magnetization of the bulk material.[28]

The spectra of Figs. 10 and 11 have been least-squares fitted, assuming a distribution of total internal magnetic fields, superimposed on a broad background, in order to simulate relaxation effects.[28] For Fe_{11}, an average internal field of $H_n\cong 430$ kOe is observed, while for $Fe_{16}Mn$ this value is reduced to 400 kOe. This reflects higher d-electron localization in the smaller Fe_{11} cluster compared to $Fe_{16}Mn$, in agreement with the trend observed in Stern-Gerlach experiments on free iron clusters and theoretical calculations.[11]

A close comparison of Figs. 10 and 11 indicates that, in going from $H_0=60$ kOe to $H_0=80$ kOe, the center of the distribution of the internal fields remains unaffected, but the detailed shape of the distribution and, therefore, that of the local magnetic moments, changes for the Fe_{11} clusters, while that of $Fe_{16}Mn$ exhibits a slight broadening but otherwise remains undisturbed. In the 80-kOe Mössbauer spectra of Fe_{11}, wings at the outer absorption lines appear, indicated by the arrows in Fig. 10(a). The observed changes in the internal field distributions in Fig. 10(b) to higher and lower internal magnetic field values are consistent with the onset of local spin polarization along the applied magnetic field, a behavior reminiscent of antiparallel-spin-coupled iron molecular paramagnetic complexes where, due to spin colinearity, an increasingly resolvable separation of spin-up (relative to $\mathbf{H}_o$) and spin-down magnetic subspectra is produced with increasing values of the applied field.[45] Thus, the Fe_{11} cluster

seems to be at the boundary of molecular–solid-state magnetic behavior, while the $Fe_{16}Mn$ cluster clearly exhibits "particlelike" magnetic behavior. The onset of local spin polarization for Fe_{11} at 80-kOe applied field coincides with the step in the magnetization vs applied-magnetic-field behavior of Fig. 7(a).

The Mössbauer spectra of the lower-dimensional clusters $[Fe_{18}S_{30}]$ (cluster 3) and $[Fe_{20}Se_{38}]$ (cluster 4) were examined in zero field at 1.6–180 K and in a longitudinally applied magnetic field of 80 kOe at 4.2 K. Mössbauer spectra obtained for the two clusters were very similar. Zero-field spectra at 4.2 K for cluster 3 are shown in Fig. 12(a) and consist of two apparent overlapping doublet features. The minority component appears as a shoulder on the positive velocity side. No magnetic hyperfine structure was observed even at 1.6 K, the lowest temperature studied. Spectral fits based on a two-site model give an isomer shift of $\delta_1=0.30$ mm/sec and a quadrupole splitting of $\Delta E_{Q1}=0.81$ mm/sec for the majority iron component, and $\delta_2=0.46$ mm/sec and $\Delta E_{Q2}=1.49$ mm/sec for the minority component. It is a mixed-valence, even-electron system, having formally $14Fe^{3+}$ and $4Fe^{2+}$ ions. In the Mössbauer spectra no individual ferrous sites, for which $\delta=0.5$–0.77 mm/sec and $\Delta E_Q \approx 3$ mm/sec, are observed. The cluster is electronically delocalized.[17]

Zero-field Mössbauer spectra of cluster 4 (not shown) are very similar to that of cluster 3, with Mössbauer parameters of majority and minority components $\delta_1=0.38$ mm/sec, $\Delta E_{Q1}=0.60$ mm/sec, and $\delta_2=0.43$ mm/sec, $\Delta E_{Q2}=1.15$ mm/sec, respectively.[20] This cluster is also of mixed valence of formally $18Fe^{3+}$ and $2Fe^{2+}$ ions. Electronic delocalization is also observed here. The spectrum of cluster 4 in a longitudinally applied magnetic field of 80 kOe at 4.2 K is shown in Fig. 12(b). This spectrum is characteristic of a diamagnetic ground-spin complex as the field observed at the iron sites equals that of the applied field H_0. Spectra of cluster 3 looked identical to those of cluster 4. Susceptibility measurements also indicate diamagnetic ground total spin states $S_T=0$, for both complexes.[20]

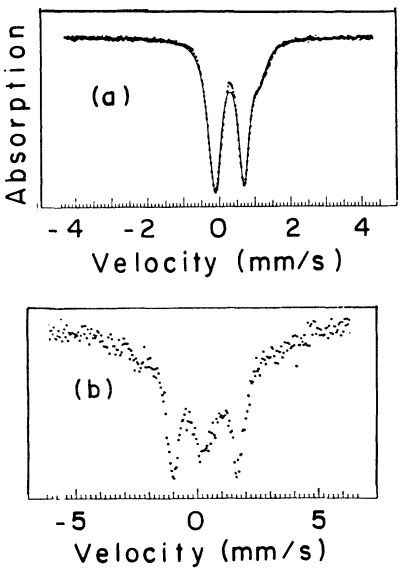

FIG. 12. (a) Mössbauer spectra of polycrystalline $(Pr_4N)_6Na_4Fe_{18}S_{30}\cdot 14MeCN$ at $T=4.2$ K. The solid line is a least-square fit to the superposition of two quadrupole doublets (see text). (b) Mössbauer spectra of polycrystalline $(Bu_4N)_{4.5}Na_{13.5}Fe_{20}Se_{38}\cdot 2PhNHCOMe\cdot 15EtOH$ at $T=4.2$ K and $H_o=80$ kOe parallel to the γ ray.

Even though the number of iron ions in compounds 3 and 4 exceed 10, no magnetic hyperfine interactions indicating the presence of collective magnetic correlations among iron spins are observed in the Mössbauer spectra. We attribute this to the fact that the Fe-Fe exchange interactions present in both of these molecules are of lower dimensionality. No magnetic exchange pathways exist to cross link rings in cluster 4 and thus this cluster remains of lower magnetic dimensionality even though topologically it is a three-dimensional structure, unlike cluster 3, which is topologically as well as magnetically lower dimensional. Any short-range magnetic correlations, if sustainable by these structures, must have a relaxation frequency $\nu \gg \nu_L$, the Larmor precession frequency of the Fe^{57} nucleus, which is of the order of 10^8 sec^{-1}.

V. CONCLUSION

Mössbauer spectroscopy, with a short characteristic measuring time of $\sim 10^{-8}$ sec, has provided experimental evidence of the presence of intramolecular short-range magnetic order within the $[Fe_{11}]$ and $[Fe_{16}Mn]$ cores of compounds 1 and 2 with a 3D magnetic exchange interaction network among iron spins. Owing to the extremely small size of the magnetic domain of compounds 1 and 2, about 10 Å in diameter, superparamagnetic-relaxation phenomena dominate the Mössbauer spectral behavior and foreclosed observation of intramolecular magnetic ordering by magnetic susceptibility methods with a signal averaging time of 1 sec or longer. These systems have provided the first experimental confirmation, to the author's knowledge, of the onset of collective magnetic phenomena associated with the solid state in molecular systems of nanometer size containing a number of interacting spins of the order of 10, as initially predicted by theoretical studies in metallic clusters.[7]

In contrast, no evidence of magnetic correlation effects were observed in the magnetically lower-dimensional systems $[Fe_{18}S_{30}]$ or $[Fe_{20}Se_{38}]$. This, however, does not necessarily disprove theoretical predictions that finite antiferromagnetic chains or rings ought to exhibit magnetic correlation effects and be able to sustain spin-wave spectra approximating those of the infinite chain as discussed in the introduction.[24] Rather, it points to the need of an even faster spectroscopic tool, such as neutron scattering and/or even lower sample temperatures in order to probe further magnetic correlations in these systems.

ACKNOWLEDGMENTS

The generous contribution of compounds 1 and 2 by S. J. Lippard of MIT and compounds 3 and 4 by R. H. Holm of Harvard University and associated crystallographic data are gratefully acknowledged. The author wishes to thank R. B. Frankel for his contribution at the

initial phase of this investigation. Special thanks go to S. Gorun, W. Micklitz, R. L. Rardin, and J. F. You for numerous discussions on the synthesis and x-ray structural characterization of these compounds. The high-field magnetization measurements were performed with the assistance of S. Foner and E. J. McNiff of the Francis Bitter National Magnet Laboratory high-field user's facility. This work was supported by the Office of Naval Research.

[1]J. R. Anderson, *Structure of Metallic Catalysts* (Academic, New York, 1975); J. H. Sinfelt, in *Annual Review of Materials Science,* edited by R. A. Higgins, R. H. Bube, and R. W. Roberts (Annual Reviews, Palo Alto, CA, 1972); E. L. Meutterties, T. N. Rhodin, E. Band, C. F. Brucker, and W. R. Pretzer, Chem. Rev. **79**, 91 (1979); *The Physical Basis of Heterogeneous Catalysis,* edited by E. Grauglis and R. J. Jaffee (Plenum, New York, 1975).

[2]K. Bittler and W. Ostertag, Angew, Chem. Int. Ed. Engl. **19**, 190 (1980).

[3]P. Ball and L. Garwin, Nature **355**, 761 (1992); G. D. Stucky and J. E. MacDougall, Science **247**, 669 (1990), and references therein.

[4]D. R. Salahub and R. P. Messmer, Surf. Sci. **106**, 415 (1981); B. Delley, A. J. Freeman, and D. E. Ellis, Phys. Rev. Lett. **50**, 488 (1983); J. Bernholc and N. A. W. Holzwartoh, *ibid.* **50**, 1451 (1983); H. Adachi, M. Tsukada, and C. Satoko, J. Phys. Soc. Jpn. **45**, 875 (1978); D. R. Salahub and F. Raatz, Int. J. Quantum. Chem. **18**, 173 (1984); J. Demuynch, M. M. Rhomer, A. Stich, and A. Veillard, J. Chem. Phys. **75**, 3443 (1981); R. C. Baetzold and R. E. Mack, *ibid.* **62**, 1513 (1975), K. Lee, J. Calloway, and S. Dhar, Phys. Rev. B **30**, 1724 (1984); G. M. Pastor, J. Dorantes-Dávila, and K. H. Bennemann, *ibid.* **40**, 7642 (1989); P. J. Jensen, S. Mukherjee, and K. H. Bennemann, Z. Phys. D **21**, 349 (1991).

[5]M. G. Mason, Phys. Rev. B **27**, 748 (1983), and references therein; S. Raaen and M. Strongin, *ibid.* **32**, 4289 (1985); C. Brechignac, M. Boyer, Ph. Cahuzac, G. Delacretaz, P. Labastie, J. P. Wolf, and L. Wöste, Phys. Rev. Lett. **60**, 275 (1988); W. Eberhardt, P. Fayet, D. M. Cox, Z. Fu, A. Kaldor, R. Sherwood, and D. Sondericker, *ibid.* **64**, 780 (1990); K. E. Schriver, J. L. Persson, E. C. Honea, and R. L. Whetten, *ibid.* **64**, 2539 (1990); K. D. Kolenbrander and M. L. Mandich, *ibid.* **65**, 2169 (1990).

[6]R. P. Messmer, S. K. Knudson, K. H. Johnson, J. B. Diamond, and C. Y. Yang, Phys. Rev. B **13**, 1396 (1976).

[7]C. Y. Yang, K. H. Johnson, D. R. Salabub, K. Kaspar, and R. P. Messmer, Phys. Rev. B **24**, 5673 (1981). More recent calculations using a tight-binding Hubbard Hamiltoinan in the unrestricted Hartree-Fock approximation by Pastor, Dorantes-Dávila, and Bennemann (see Ref. 4) also agree with these predictions.

[8]G. C. Shull and H. A. Mook, Phys. Rev. Lett. **16**, 184 (1966).

[9]W. A. de Heer, P. Milani, and A. Chatalain, Phys. Rev. Lett. **65**, 488 (1990); *Elemental and Molecular Clusters,* edited by G. Benedek, T. P. Martin, and G. Pacchioni (Springer, Berlin, 1988); J. J. Krebs, P. Lubitz, A. Chaiken, and G. A. Prinz, Phys. Rev. Lett. **63**, 1645 (1989); B. Heinrich, Z. Celinski, J. F. Cochran, W. B. Muir, J. Rudo, Q. M. Zhong, S. Arrott, and K. Myrtle, *ibid.* **64**, 673 (1990); *Microclusters,* edited by S. Sugano, Y. Nishina, and S. Ohnishi (Springer, Berlin, 1987); E. S. Smotkin *et al.*, Chem. Phys. Lett. **152**, 265 (1988); M. L. Steigerwald and E. L. Brus, Ann. Rev. Mater. Sci. **19**, 471 (1989).

[10]O. Cheshnovsky, K. J. Taylor, J. Conceicao, and R. E. Smalley, Phys. Rev. Lett. **64**, 1785 (1990); A. M. Thayer, M. L. Steigerwald, T. M. Duncan, and D. C. Douglan, *ibid.* **60**, 2673 (1988).

[11]D. M. Cox, D. J. Trevor, R. L. Whetten, E. A. Rohlfing, and A. Kaldor, Phys. Rev. B **32**, 7290 (1985); J. Merikoski, J. Timonen, M. Manninen, and P. Jena, Phys. Rev. Lett. **66**, 938 (1991), and references therein.

[12]J. P. Bucher, D. C. Douglass, and L. A. Bloomfield, Phys. Rev. Lett. **66**, 3052 (1991); J. P. Bucher, D. C. Douglas, P. Xia, B. Hayens, and L. A. Bloomfield, Z. Phys. D **19**, 251 (1991).

[13]S. M. Gorun and S. J. Lippard, Nature **319**, 666 (1986).

[14]S. M. Gorun, G. C. Papaefthymiou, R. B. Frankel, and S. J. Lippard, J. Am. Chem. Soc. **109**, 3337 (1987).

[15]W. Micklitz and S. J. Lippard, J. Am. Chem. Soc. **111**, 6856 (1989).

[16]G. Schmid, Polyhedron **7**, 2321 (1988); A. Ceriotti, F. Demartin, G. Langoni, M. Manassero, M. Marchionna, G. Pira, and M. Sansoni, Angew. Chem. Int. Ed. Engl. **24**, 697 (1985).

[17]J. F. You, B. S. Snyder, G. C. Papaefthymiou, and R. H. Holm, J. Am. Chem. Soc. **112**, 1067 (1990), and references cited therein.

[18]K. L. Taft and S. J. Lippard, J. Am. Chem. Soc. **112**, 9629 (1990).

[19]J. F. You and R. H. Holm, Inorg. Chem. **30**, 1431 (1991).

[20]J. F. You, G. C. Papaefthymiou, and R. H. Holm, J. Am. Chem. Soc. **114**, 2697 (1992).

[21]G. C. Papaefthymiou, in *Clusters and Cluster-Assembled Materials,* edited by R. S. Averback, J. Bernholc, and D. L. Nelson, MRS Symposia Proceedings No. 206 (Materials Research Society, Pittsburgh, 1991), p. 539.

[22]L. J. de Jongh and A. R. Miedema, Adv. Phys. **23**, 1 (1974).

[23]J. Van Kranendouk and J. H. Van Vleck, Rev. Mod. Phys. **30**, 1 (1958).

[24]J. des Cloizeaux and J. J. Pearson, Phys. Rev. **128**, 2131 (1962).

[25]J. C. Bonner and M. E. Fisher, Phys. Rev. **135**, A640 (1964).

[26]F. Liu, S. N. Khanna, and P. Jena, Phys. Rev. B **42**, 976 (1990); F. Liu, M. R. Press, S. N. Khanna, and P. Jena, *ibid.* **39**, 6914 (1989).

[27]W. F. Brown, Jr., J. Appl. Phys. **30**, 1305 (1959).

[28]D. G. Rancourt, Hyperfine Interact. **40**, 183 (1988).

[29]M. F. Thomas, in *Mössbauer Spectroscopy Applied to Inorganic Chemistry,* edited by Gary J. Long (Plenum, New York, 1987), Vol. 2, p. 209.

[30]T. G. Spiro, S. E. Allerton, J. Denner, A. Terzis, R. Bils, and P. Saltman, J. Am. Chem. Soc. **88**, 2721 (1966); B. A. Sommer, D. W. Margerum, J. Reuner, P. Saltman, and T. G. Spiro, Bioinorg. Chem. **2**, 295 (1973).

[31]S. M. Gorun, in *Metal Clusters in Proteins,* edited by L. Que, Jr. (American Chemical Society, Washington, D.C., 1988), Chap. 10, p. 196, and references cited therein; S. J. Lippard, Angew. Chem. Int. Ed. Engl. **27**, 344 (1988), and references cited therein.

[32]E. C. Theil, Annu. Rev. Biochem. **56**, 289 (1987).

[33]S. H. Yang, C. L. Pettiette, J. Conceicao, O. Cheshnovsky, and R. E. Smalley, Chem. Phys. Lett. **139**, 233 (1987); W. Krätschmer, L. D. Lamb, K. Fostiropoulos, and D. R. Huffman, Nature **347**, 354 (1990).

[34]M. Blume, Phys. Rev. Lett. **18**, 305 (1967).

[35]J. M. D. Coey, Phys. Rev. Lett. **27**, 1140 (1971); M. F. Thomas and C. E. Johnson, in *Mössbauer Spectroscopy,* edited by D. P. E. Dickson and F. T. Berry (Cambridge University Press, Cambridge, 1986), Chap. 4, p. 143; Q. A. Parkhurst, C. E. Johnson, and M. F. Thomas, J. Phys. C **18**, 3249 (1985); A. E. Berkowitz, J. A. Lahut, I. S. Jacobs, L. M. Levinson, and D. W. Forestor, Phys. Rev. Lett. **34**, 594 (1975).

[36]R. B. Frankel, in *Mössbauer Effect Methodology,* edited by J. Gruverman, C. W. Siedel, and D. K. Dieterly (Plenum, New York, 1974), Vol. 9, p. 151.

[37]A. P. Ginsberg, Inorg. Chim. Acta. Rev. **5**, 45 (1971).

[38]R. L. Carlin, *Magnetochemistry* (Springer-Verlag, New York, 1985).

[39]K. S. Murray, Coord. Chem. Rev. **12**, 1 (1974); D. M. Kurtz, Jr., Chem. Rev. **90**, 585 (1990).

[40]W. Kundig, H. Bömmel, G. Constabaris, and R. H. Linquist, Phys. Rev. **142**, 327 (1966); K. S. Kaufman, G. C. Papaefthymiou, R. B. Frankel, and A. Rosenthal, Biochim. Biophys. Acta **629**, 522 (1980).

[41]S. Mørup, H. Topsoe, and J. Lipka, J. Phys. **51**, 6 (1976); G. D. Watt, R. B. Frankel, G. C. Papaefthymiou, K. Spartalian, and E. I. Stiefel, Biochemistry **25**, 4330 (1986).

[42]N. N. Greenwood and T. C. Gibb, *Mössbauer Spectroscopy* (Chapman and Hall, London, 1971).

[43]C. Kittel, *Introduction to Solid State Physics* (Wiley, New York, 1966); G. Burns, *Solid State Physics* (Academic, New York, 1985); A. H. Morrish, *The Physical Principles of Magnetism* (Wiley, New York, 1965).

[44]W. H. Armstrong, A. Spool, G. C. Papaefthymiou, R. B. Frankel, and S. J. Lippard, J. Am. Chem. Soc. **106**, 3653 (1984).

[45]J. J. Girerd, G. C. Papaefthymiou, A. D. Watson, E. Gamp, K. S. Hagen, N. Edelstein, R. B. Frankel, and R. H. Holm, J. Am. Chem. Soc. **106**, 5941 (1984). A typical example for a high-spin ferric-trimer-complex Mössbauer spectrum in an external magnetic field is shown in Fig. 6 of this reference. This type of behavior may be taken as the Mössbauer signature of an antiparallel-spin-coupled iron molecular paramagnet.

[46]R. E. Vandenberghe and E. De Grave, in *Mössbauer Spectroscopy Applied to Inorganic Chemistry,* edited by G. J. Long and F. Grädjean (Plenum, New York, 1989), Vol. 3, p. 59.

[47]D. Chowdhury, *Spin Glasses and Other Frustrated Systems* (Princeton University Press, Princeton, NJ, 1986); C. M. Hurd, Contem. Phys. **23**, 469 (1982).

[48]The dipole-dipole interaction energy $\mu_1 \cdot \mu_2 / r^3 \sim 10^{-20}$ ergs for two magnetic dipoles of $1\mu_B$ each separated by a distance $r = 20$ Å, which is much weaker than either thermal energies $k_B T$ for the lowest temperature used in these expeirments, or the orientation energy of each dipole $-\mu \cdot \mathbf{H}_o$ in the external field of 80 kOe, both of which are of the order of 10^{-16} ergs.